European Journal of Material Science 10 (1), 37-52, 2022
Print ISSN: ISSN 2055-6551(Print),
Online ISSN: ISSN 2055-656X (Online)
Website: https://www.eajournals.org/
Publication of the European Centre for Research Training and Development UK

# Austenite Grain Refinement of Ductile Iron Castings

**Michael Adeniyi**
Georgia Southern University/Department of Mechanical Engineering Statesboro GA
Email: adeniyitobi01@gmail.com

doi.org/10.37745/ejms.2014/vol10n13752 Published December 02, 2024

**Citation**: Adeniyi M. (2024) Austenite Grain Refinement of Ductile Iron Castings, *European Journal of Material Science* 10 (1), 37-52

**Abstract:** *Austenite is the strong phase that contributes most to the strength of an iron alloy. Therefore, for a ductile iron to be strengthened the austenite phase must be strengthened, and one main approach is by controlling its nucleation and growth during solidification. The effect of a selected amounts of titanium addition on austenite grain refinement in ductile iron will be determined in this study using three methods: secondary dendrite arm spacing measurement, measurement of the nodule count of graphite particles and liquidus undercooling and recalescence measurement. Titanium addition in the amount of 0.02wt.% was tested. The results showed that addition of titanium did have an impact on the fineness of the dendrite arms closer to the casting wall but the result was quite similar to the addition without titanium at the thin section of the casting. Farther away from the casting wall, the titanium modified heat grew coarser and sparse. The nodule count result showed that generally, the nodule count dropped due to the addition of titanium and this can reduce the material's ductility. The results from the liquidus recalescence measurement needs to be reviewed with a higher sample rate to obtain a better understanding of the recalescence at the liquidus temperature at the thin section of the casting.*

**Keywords**: ductile iron, grain refinement, titanium, austenite nucleation

## INTRODUCTION

The goal of this study is to examine refining austenite in ductile iron castings when a heterogenous nucleation approach is adopted. Refined austenite grain structure in ductile iron helps to improve its mechanical property and leads to higher strength and ductility in ductile iron castings. Ductile iron consists of small, round, spherical nodules of graphite in an iron matrix. Ductile iron consists of a measure of magnesium which reacts with oxygen and sulfur in the melt to dissolve carbon in a spherical form. This form possesses better strength and ductility over gray iron. (G. M. Goodrich 2018). Austenite is the proeutetic phase in hypoeutectic ductile irons, and it forms a dendritic shape from the graphite nodules. The interdendritic space will be occupied by eutectic structures consisting of austenite and graphite from eutectic cooling.

The austenite is composited with the eutectic mixture, and it is the stronger phase which makes a dominant contribution to the strength of iron alloy. Therefore, ductile iron can be strengthened if

the austenite is strengthened. A technique to strengthen the austenite is to refine the austenite grain size and this can be achieved by regulating the growth of austenite during cooling. Heterogeneous nucleation of austenite leads to finer austenite grain size, and also expands the equiaxed zone in castings. This leads to more even grain structure in castings and consequently improve the property of the castings. The morphology of cast iron depends on the iron components, cooling rate and inoculating agent during solidification. Higher carbon and/or silicon concentration, slower solidification cooling rates, and the presence of additional elements all promote graphite formation. Alternatively, carbide formation is promoted by low carbon and/or silicon concentrations, presence of certain elements, and faster solidification cooling rate. Compositions with a low carbon and/or silicon content, appropriate carbide forming alloying additions, or the addition of carbide-promoting components that prevent graphite formation are necessary for the creation of white irons. The existence of nuclei in the liquid metal is a crucial factor in regulating the microstructure during solidification. These nuclei are able to induce graphite formation in ductile, compacted graphite, and gray irons. After nucleation, the graphite shape is regulated during growth. (G.M. Goodrich 2008a).

Solidification of a phase begins with the appearance of a substrate from which the phase can form. This substrate will introduce graphite formation as proeutectic graphite in hypereutectic composition or as graphite phase in hypoeutectic composition. The substrate may be added to the melts during melting as inoculants. Inoculants amounts in the range of 0.1-0.5% are used to minimize white iron formation and improve graphite formation. Inoculation raises the nodule count in ductile iron and compacted graphite irons and encourages the production of type A flake graphite in gray irons (often with an increase in the number of eutectic cells). Inoculation is not regarded as alloying because the inoculants' nucleating effect wears off over time. Additives to molten iron may be made with the goal of preventing graphite from forming during solidification. In order to increase the section thickness within which white iron can be made, it is a common practice in the formation of malleable iron to add trace amount of bismuth or tellurium. This causes the material to solidify completely as white iron without any mottle or free graphite present. (G.M. Goodrich 2008a).

This study investigates austenite grain refinement through the introduction of titanium addition by heterogeneous nucleation approach and it is assumed that titanium addition will act suitably as nucleation agent for austenite. The strengthening will be beneficial to industries such as transportation industry for reducing the weight of their components and increasing the strength-to-weight-ratio. This makes ductile iron more competitive and appealing to materials designers in comparison to aluminum and steel. It has been studied that titanium addition refined the austenite grain size in steel (Adabavazeh, Hwang, and Su 2017). It is expected that titanium addition will refine the austenite grain structure of ductile iron and austenite grain refinement of ductile iron will improve the strength and ductility of the iron. Too much of the addition may be harmful to the graphite phase morphology of ductile iron. The effect of 0.02wt.% of titanium addition will be studied. The effectiveness of this addition on the microscopic structure and properties of ductile iron casting will be measured using three main techniques: liquidus recalescence measurement, measurement of the secondary dendrite arm spacing and measurement of the nodule count of graphite particles.

European Journal of Material Science 10 (1), 37-52, 2022
Print ISSN: ISSN 2055-6551(Print),
Online ISSN: ISSN 2055-656X (Online)
Website: https://www.eajournals.org/
Publication of the European Centre for Research Training and Development UK

## MATERIALS AND METHODS

### Materials

Optical Emission Spectrometer

An optical emission spectrometer was used along with chilled samples from both the melting furnace and ladle (after magnesium treatment) in order to adjust and attain the expected final chemistry of the casting.

Thermocouple and Data Acquisition system and recording software

A Data Acquisition system and recording software was used in obtaining cooling curve data for the heats along with K-type thermocouples. This data was used in obtaining the measurement of recalescence of the liquidus temperature for the various additions.

Mold Type

No bake mold because of its durability and ability to be used without a flask

Furnace type

The furnace type used for this research was a 100-pound medium frequency induction furnace in order to attain precise pouring and temperature control

Table 1: Proposed chemistry of the casting

| Element | C | Si | Mn | Ni | Mo | Mg |
|---|---|---|---|---|---|---|
| Wt. % | 3.5 | 2.0 | 1.0 | 1.0 | 0.1 | 0.03-0.04 |

### Heating and Pouring Procedure

The effect of titanium addition in relation to the base inoculant was compared at the thin and thick section of the casting wall using three methods: dendrite arm spacing measurement, nodule count of graphite particles and liquidus recalescence measurement. Three molds were poured, two keel block molds (ASTM A536 keel blocks) and one insulated sleeve mold. Two thermocouples were instrumented to each of the keel block mold at height of 10mm and 50.8mm respectively from the bottom surface of the keel- block mold and one thermocouple was instrumented at a height of 76.2mm from the bottom surface of the insulated sleeve mold. The first keel block contained the charge plus the baseline inoculant (Alinoc), the second keel block mold and the insulated sleeve mold contained the charge plus the base inoculant (Alinoc) plus 0.02wt.% titanium addition. The addition amount of titanium for each mold can be seen in Table 2.

Table 2: Inoculant and additions for the various molds

| | **Inoculant and Addition** |
|---|---|
| Mold 1 (Keel-block mold) | ALINOC |
| Mold 2 (Keel-block mold) | ALINOC + 0.02 wt.% Ti |
| Mold 3 (Insulated sleeve mold) | ALINOC + 0.02 wt.% Ti |

A base inoculant and nodulizer was needed to stabilize the spheroidal graphite particles in the heat. ALINOC inoculant which contains silicon, aluminum and calcium was employed. The composition of ALINOC inoculant are listed in Table 3. It was also employed in a heat without the titanium addition to establish a good baseline for the comparison.

Table 3: Alinoc Inoculant composition in wt.%

| | Si | Ca | Al |
|---|---|---|---|
| ALINOC | 66.63 | 0.97 | 4.15 |

**Melting and pouring**

The charge material based on Table 4 were melted in the induction furnace, the melt was heated up to about 1350 $^{o}$C, then the melt surface was deslag and a lollipop sample was taken from the furnace for chemical analysis to adjust and attain the expected chemistry of the casting using the optical emission spectrometer. Once the melt reached a temperature of 1430 $^{o}$C, a pre-heated ladle was transferred to the induction furnace and the nodulizer and alinoc inoculant was added into the ladle. The furnace was tapped into the ladle at 1430 $^{o}$C after-which the ladle surface was deslag and a lollipop sample was taken from the ladle for chemical analysis. The heat was then poured from the ladle into the first keel block mold after-which 3.2g of titanium was added to the ladle and the heat from the ladle was then poured to the second keel block mold and the insulated sleeve mold respectively.

Table 4: Charge table with Alinoc Inoculant

| Charge | Weight (kg) | Weight (lbs) |
|---|---|---|
| TF-10 Sorel Metal | 25.6 | 56.44 |
| Fe75Si | 0.485 | 1.07 |
| FeMn | 0.45 | 0.99 |
| Steel Scrap (1018) | 4.430 | 9.77 |
| FeMo | 0.045 | 0.1 |
| Ni | 0.32 | 0.71 |
| Total charge | 31.33 | 69.08 |
| **(Base Inoculant): In-ladle** | | |
| Nodulizer | 0.439 | 0.97 |
| Alinoc Inoculant | 0.0476 | 0.105 |

The chemical compositions of the heat from the furnace and ladle after treatment can be seen in Table 5.

Table 5: Heat Chemistries from the ladle and furnace

| | C | Si | Mn | Mo | Ni | Al | Ti | Mg |
|---|---|---|---|---|---|---|---|---|
| Furnace | 3.54 | 1.31 | 1.02 | 0.10 | 1.01 | 0.001 | 0.009 | ~ |
| Ladle | 3.45 | 2.06 | 1.05 | 0.16 | 1.07 | 0.015 | 0.011 | 0.042 |

**Measurement of the Secondary Dendrite Arm Spacing**

In order to evaluate how the alloy additions affected the austenite structure, three techniques were applied which are: measurement of the secondary dendrite arm spacing, measurement of the nodule count of graphite particles and measurement of the liquidus recalescence temperature. The secondary dendrite arm spacing measurement was done at the tensile region of the keelblock. Metal samples were sectioned from the tensile region of the keel-block, the first region (1inch from the bottom of the keel-block) depicts the thin section, the second region (1inch directly above the first region) depicts the thick section. Each of these regions were given number specification. After-which a mounting press was used to mount the metal samples into a bakelite, and the samples were later grinded, polished, and etched in order to reveal the matrix structure. The samples were etched with 2vol.% nital in order to examine the dendrite arms using a Zeiss microscope. The micrographs were captured from the microscope and the secondary dendrite arm spacing were evaluated and calculated using the ImageJ application software. The secondary dendrite arm spacing is dependent on the cooling rate of castings, and the cooling rate of casting reduces farther away from the surface of the casting, it was important to capture the micrograph at an increasing interval from the surface of the casting. This provided a good understanding of the measure of the grain size fineness all through the tensile specimen. To measure the secondary dendrite arm spacing using the imagej application software, the distance measure function of the image was used. A line was drawn across three or more dendrite arms, and the length of the line in addition to the amount of dendrite arms crossed were recorded. To determine the average dendrite arm spacing, the sum of all line lengths was divided by the total amount of dendrite arms crossed for each region.

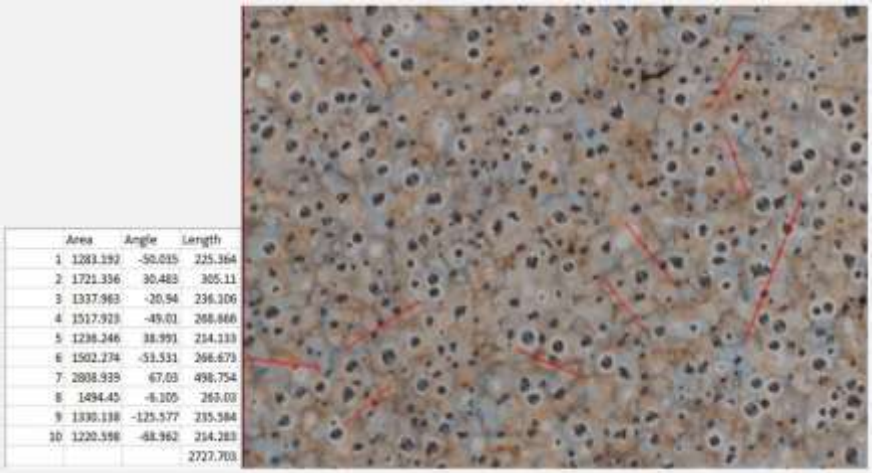


Figure 1: Measurement of the secondary dendrite arm spacing at a specific region of the keel block

**Measurement of Nodule Count of Graphite Particles**

The samples right after polishing were taken to the microscope in order to analyze the nodule count of the graphite particles before etching. The micrographs were captured from the microscope and the nodule count were analyzed using the imagej's brightness threshold function. Nodule count was measured in each of the tensile specimen at increasing distances from the casting wall. The amount of graphite nodules per square millimeter in each region were obtained by counting all particles with an area larger than 20μm$^2$ and a circularity more than 50% at increasing distances from the casting wall.

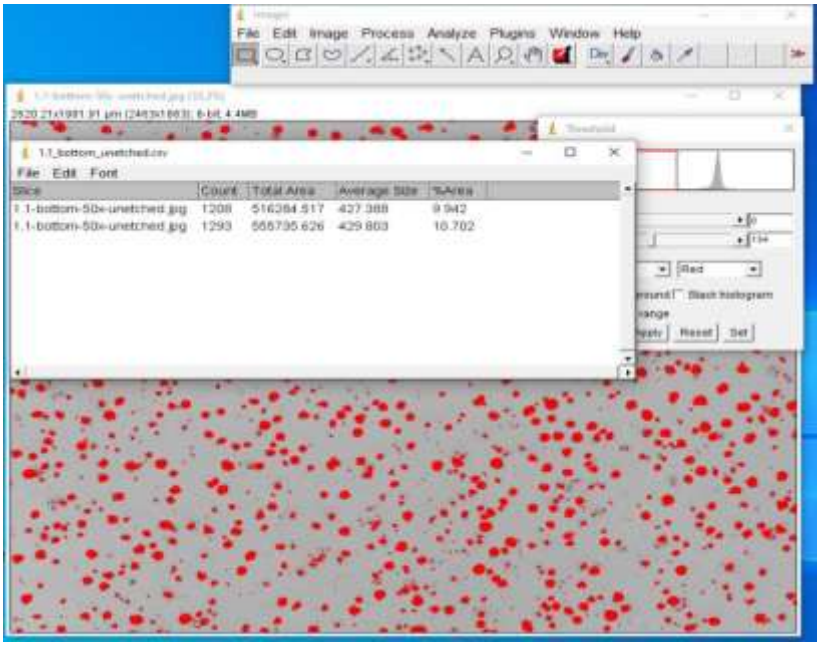


Figure 2: Sample measurement of the nodule count of graphite particles

European Journal of Material Science 10 (1), 37-52, 2022
Print ISSN: ISSN 2055-6551(Print),
Online ISSN: ISSN 2055-656X (Online)
Website: https://www.eajournals.org/
Publication of the European Centre for Research Training and Development UK

### Measurement of the Liquidus Recalescence Temperature

The measurement of the liquidus recalescence temperature were taken from the two keel block molds and the insulated sleeve mold. For the keel block molds, two thermocouples were instrumented at height of 10mm and 50.8mm respectively from the bottom surface of each of the keel block molds. The insulated sleeve mold was prepared by inserting an insulating sleeve into a no-bake sand mold. A thermocouple was instrumented through the mold and the sleeve up to the centre of the sleeve at an height of 76.2mm from the bottom surface of the insulated sleeve mold. The insulated sleeve was added in order to verify the results of a previous research. The molds were poured and the cooling curve data of the respective pours were collected through the thermocouples using a data acquisition and recording software. This experiment was done in order to investigate the measure of recalescene at the liquidus temperature of the alloy. A lower recalescence temperature of the mold with the titanium alloy addition compared to the mold with the solely base inoculant depicts a better inoculation or better heterogeneous nucleation with titanium addition and on the other hand a higher recalescence temperature depicts a bad inoculation.

Figure 3: Insulated Sleeve mold

## RESULTS AND ANALYSIS

### Secondary Dendrite Arm Spacing Measurement

To evaluate the effect of the titanium addition on the austenite grain size, the secondary dendrite arm spacing was evaluated. The secondary dendrite arm spacing as shown in Figure 4 was measured from varying distances from the casting wall.

European Journal of Material Science 10 (1), 37-52, 2022
Print ISSN: ISSN 2055-6551(Print),
Online ISSN: ISSN 2055-656X (Online)
Website: https://www.eajournals.org/
Publication of the European Centre for Research Training and Development UK

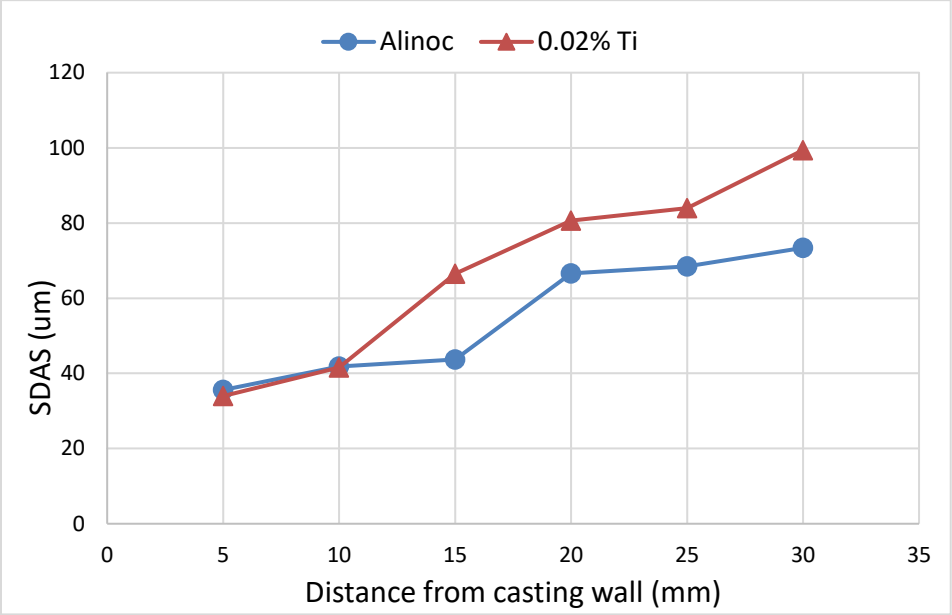


Figure 4. SDAS at varying distance of the sample from the casting wall

From the result shown, firstly, for the heat with solely Alinoc inoculant, the dendrite structure was well refined within 15mm of the casting wall but there was an increase in the size of the dendrite arms further away from the casting wall. For the heat with Alinoc and 0.02wt.% titanium addition, the dendrite arm spacing was well refined within 10mm of the casting wall, however, there was an increase in the size of the dendrite arms further away from the casting wall.

Further tests with different inoculants and different titanium amounts would be required to have a better understanding of the effect of the addition with varying amounts. There would be a critical value of titanium amount that would refine the austenite grain size in ductile iron. It can also be seen from the micrograph sample in figure 10 and 11 that the dendrites arms were much coarser beyond 10mm of the casting wall for the heat with titanium addition in comparison to the heat without titanium.

The micrograph for each of the sections tested on the keel block is shown in Figures 5 and 6. The left micrograph was taken 1inch from the bottom of the keel block while the right micrograph was taken 1inch directly above the first region. Lower dendrite arm spacing is seen closer to the casting wall and farther from the casting wall the dendrite arms grew bigger.

European Journal of Material Science 10 (1), 37-52, 2022
Print ISSN: ISSN 2055-6551(Print),
Online ISSN: ISSN 2055-656X (Online)
Website: https://www.eajournals.org/
Publication of the European Centre for Research Training and Development UK


Figure 5: Micrograph for the solely Alinoc addition

European Journal of Material Science 10 (1), 37-52, 2022
Print ISSN: ISSN 2055-6551(Print),
Online ISSN: ISSN 2055-656X (Online)
Website: https://www.eajournals.org/
Publication of the European Centre for Research Training and Development UK

Figure 6: Micrograph for the Alinoc + 0.02% titanium addition

European Journal of Material Science 10 (1), 37-52, 2022
Print ISSN: ISSN 2055-6551(Print),
Online ISSN: ISSN 2055-656X (Online)
Website: https://www.eajournals.org/
Publication of the European Centre for Research Training and Development UK

## Nodule Count Measurement Result

The nodule count results for each of the additions at varying distances from the casting wall can be seen in Figure 7

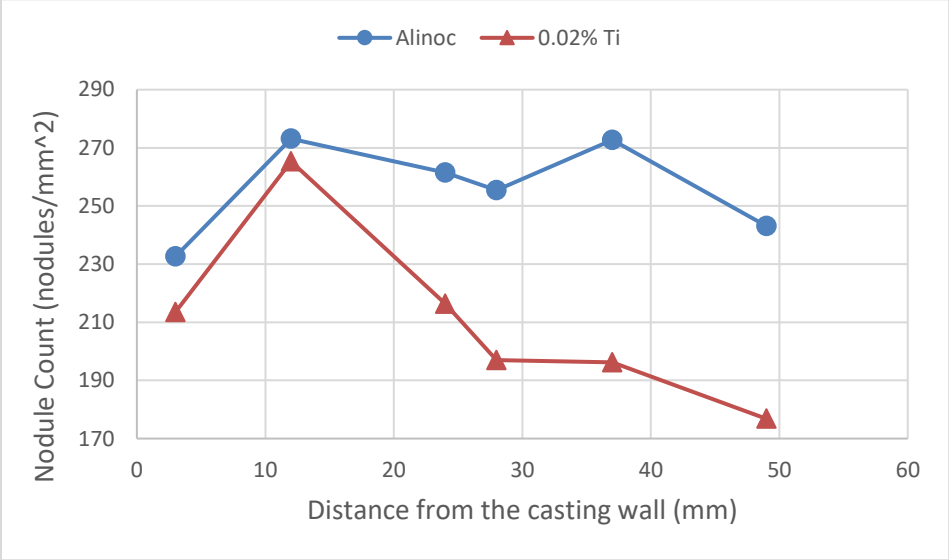


Figure 7. Nodule Count at varying distance of the sample from the casting wall

Cooling rate decreases from the surface of the casting, so it was important to access the nodule count measurement at an increasing interval from the wall of the casting. Generally, the heat with the titanium addition had a lower nodule count than the heat inoculated with solely alinoc. Both additions had a lower nodule count within 3mm of the casting wall before an increase in nodule count within 12mm of the casting wall, further from the casting wall there was a drop in nodule count, although there was an exception of an increase in nodule count within 37mm of the casting wall for the heat inoculated with solely alinoc. This could have been because of porosity within the test region as shrinkage or porosity were seen in the micrographs.

### Measurement of Liquidus Recalescence

The cooling curve for each of the additions at the thin and thick section of the casting as recorded from the thermocouples are shown in figures 8-12.

European Journal of Material Science 10 (1), 37-52, 2022
Print ISSN: ISSN 2055-6551(Print),
Online ISSN: ISSN 2055-656X (Online)
Website: https://www.eajournals.org/
Publication of the European Centre for Research Training and Development UK

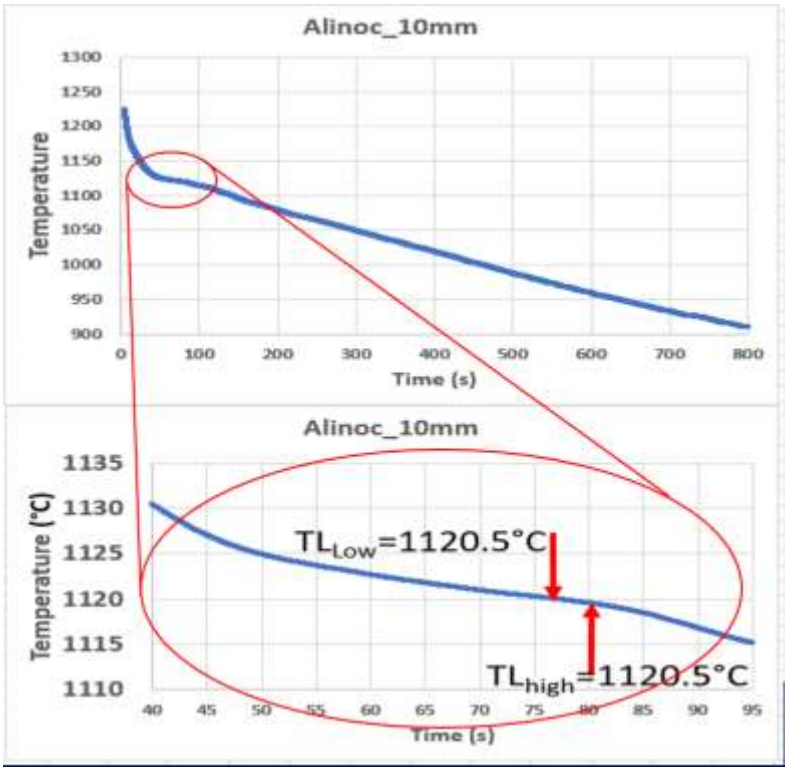


Figure 8: Recalescence at the liquidus for the solely Alinoc addition 10mm from the cast wall

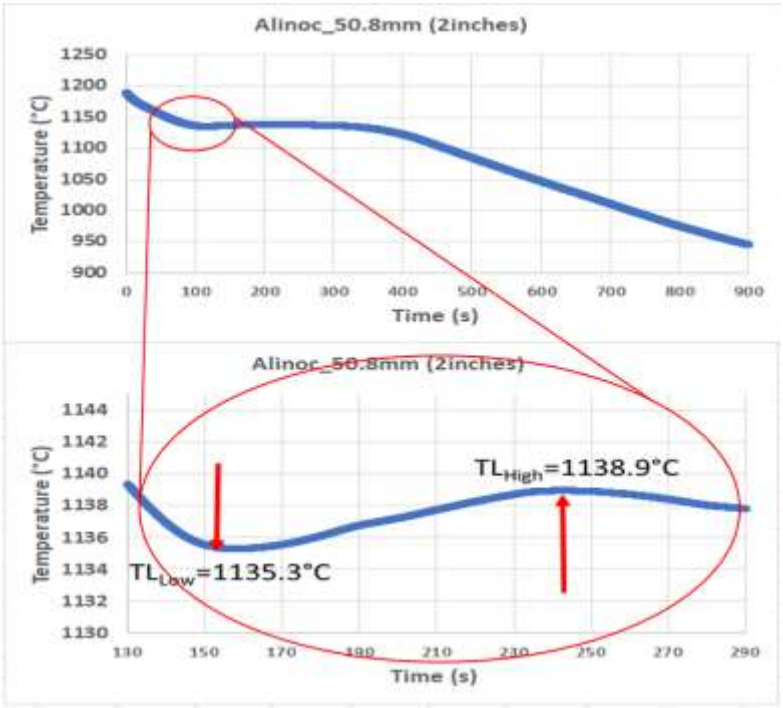


Figure 9: Recalescence at the liquidus for the solely Alinoc addition 50.8mm from the cast wall

European Journal of Material Science 10 (1), 37-52, 2022
Print ISSN: ISSN 2055-6551(Print),
Online ISSN: ISSN 2055-656X (Online)
Website: https://www.eajournals.org/
Publication of the European Centre for Research Training and Development UK

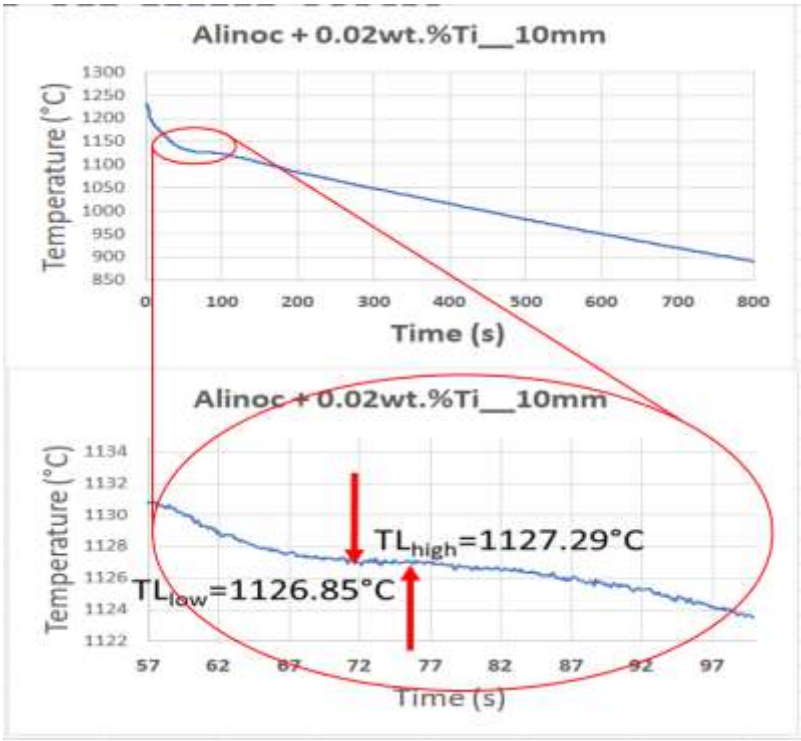


Figure 10: Recalescence at the liquidus for the Alinoc plus 0.02% Ti addition 10mm from the cast wall

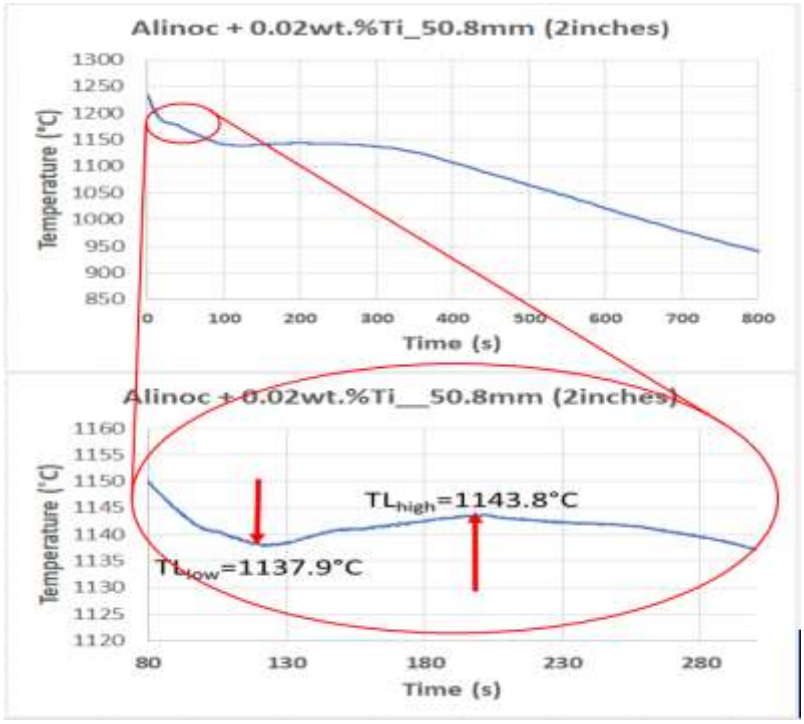


Figure 11: Recalescence at the liquidus for the Alinoc plus 0.02% Ti addition 50.8mm from the cast wall

European Journal of Material Science 10 (1), 37-52, 2022
Print ISSN: ISSN 2055-6551(Print),
Online ISSN: ISSN 2055-656X (Online)
Website: https://www.eajournals.org/
Publication of the European Centre for Research Training and Development UK

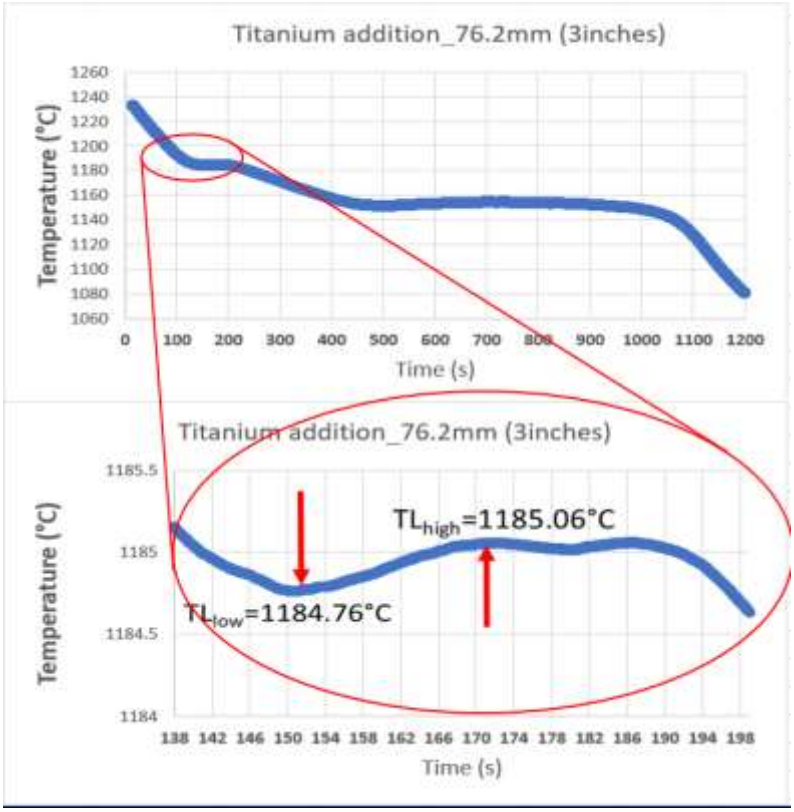


Figure 12: Recalescence at the liquidus for the insulated sleeve 76.2mm from the cast wall

The undercooling result both at 10mm and 2inches from the casting wall for the heats with solely alinoc and the 2% Ti addition can be seen in Table 6

Table 6: Liquidus recalescence temperatures

| **Addition** | **$TL_{Low}$(°C)** | **$TL_{High}$(°C)** | **$TL_{High}$- $TL_{Low}$** |
|---|---|---|---|
| Alinoc (10mm from wall) | 1120.50 | 1120.50 | 0 |
| Alinoc (50.8mm from bottom) | 1135.30 | 1138.90 | 3.60 |
| Alinoc +0.02% Ti (10mm from wall) | 1126.85 | 1127.29 | 0.44 |
| Alinoc +0.02% Ti (50.8mm from bottom) | 1137.90 | 1143.80 | 5.90 |
| Alinoc +0.02% Ti (76.2mm from bottom) | 1184.76 | 1185.06 | 0.30 |

The liquidus recalescence temperature is the temperature difference between the high and low temperatures at liquidus as seen in figures 8-12. The efficiency of an alloy as a heterogeneous inoculant should correspond with less recalescence at the temperature of the liquidus. From the measurement of the liquidus recalescence at the thin section of the casting (10mm from the casting wall), it was observed that for both

additions, it was impossible to obtain a liquidus recalescence temperature at the thin section of the casting, although a recalescence was observed for the heat with titanium addition closer to the casting wall but the result was not reliable. A sample rate of 10S/s was utilized which was too low to obtain the recalescence at the thin section of the casting. The thin section of the casting has the highest cooling rate, so to observe the recalescence at the thin section, a higher sample rate must be utilized. At the thick section of the casting (50.8mm from the casting wall), less recalescence of the liquidus temperature was observed for the heat without titanium in comparison to the titanium treated heat. This shows that titanium is not an effective austenite nucleating agent at the amount tested at the thick section of the casting. This is consistent with the result observed from the secondary dendrite arm spacing where the dendrites arms were coarser for the heat with titanium compared to the heat without titanium farther from the casting wall. The insulated sleeve cooling curve measurement was used to verify the result of a previous research and a recalescence of 0.3 ºC was observed at the thick section of the casting (76.2mm from the casting wall).

## FINDINGS AND CONCLUSIONS

### Findings

From the result obtained from the SDAS, the titanium addition did influence the fineness of the dendrite arm closer to the casting wall, but it was not much imparted as the result was still quite similar to the heat without titanium, however, farther away from the casting wall the dendrites arms grew coarser. The effects of the various addition on the fineness of the dendrite arm were highly dependent on the solidification rate because there was a sharp drop of grain fineness between the surface of the casting and farther away from the casting wall. From the nodule count result of both heats, it was observed that the titanium modified heat had a lower nodule count compared to the heat without titanium. Lower nodule count as seen with the titanium treated heat could promote the formation of carbides which can reduce the ductility of the metal. From the liquidus recalescence result, the result obtained from the thin section of the casting was not reliable, further experiment on the measure of recalescence of the liquidus at the thin section of the casting must be done with a higher sample rate for testing. The recalescence result obtained at the thick section of the casting proved consistent with the secondary dendrite arm spacing result farther away from the casting wall, it was shown that the heat with titanium addition had a higher recalescence compared to the heat without titanium at the thick section of the casting and at a slower cooling rate. This demonstrates that titanium is ineffective as an austenite nucleating agent at the thick region of the casting.

### Future Work

There are more steps that could help clarify the effect of titanium addition on ductile iron. Firstly, the recalescence of the liquidus temperature must be reviewed using a higher sample rate to ascertain the effect of the titanium addition at a faster cooling rate closer to the casting wall. Also, tensile testing analysis can also be done at the thin and thick section of the casting in order to understand the change in material properties between the heats when titanium is added. It would also be beneficial to test a wider range of titanium addition amount, only more testing would determine the critical amount of titanium that can serve as an effective nucleating agent for austenite.

## CONCLUSION

Addition of low amount of titanium refined the austenite grain size at the thin section of the casting (closer to the casting wall and at a fast-cooling rate), but farther from the casting wall and at a slow cooling rate the austenite grains grew coarser and less distinct. Therefore, low amount of titanium addition could be employed to increase the strength of light-weight ductile iron castings such as the clutch housing, the gear case assembly, engine's crankcase, oil tank of an engine etc. But this addition will not be effective on heavy duty casting such as an engine cylinder.

## REFERENCES

Barlett, L., & Bryan, A. (2016) Grain Refinement in Lightweight Advanced High- Strength Steel Castings. *International Journal of Metalcasting* 10 (4): 401–20.

Goodrich, G. M. (2008b) Ductile Iron Castings. *In Cast Iron Science and Technology* 15, 856–871. ASM International.

Goodrich, G. M. (2008a) Introduction to Cast Irons. *In Cast Iron Science and Technology* 15, 785–811. ASM International.

Adabavazeh, Z., Hwang, W., & Su, Y. (2017) Effect of adding cerium on microstructure and morphology of ce-based inclusions formed in low-carbon steel. *Scientific Reports*, 7.

Górny, M., Kawalec, M., Sikora, G., Olejnik, E., & Lopez, H. (2018) Primary structure and graphite nodules in thin-walled high-nickel ductile iron castings. *Metals*, 8(8).

Stefanescu, D. (2017a) Classification and Basic Types of Cast Iron. *In Cast Iron Science and Technology*, 12–27. ASM International.

Stefanescu, D. & Roxana, R. (2004a) Fundamentals of Solidification. *In Metallography and Microstructures*, 71–92. ASM International.

Li, X., Guangyi L., Qichen W., Jingxiao Z., Zhenjia X., & Chengjia S. (2021) The Effects of Prior Austenite Grain Refinement on Strength and Toughness of High-Strength Low-Alloy Steel. *Metals* 12 (1): 28.

Lima, F. F. O., Bauri, L. F., Pereira, H. B., & Azevedo, C. R. F. (2020) Effect of the Cooling Rate on the Tensile Strength of Pearlitic Lamellar Graphite Cast Iron. *International Journal of Cast Metals Research* 33 (4–5): 201–17.

Ohno, M., & Kiyotaka, M. (2008) Refinement of As-Cast Austenite Microstructure in S45C Steel by Titanium Addition. *ISIJ International* 48 (10): 1373–79.

Barlett, L., & Van Aken, D. (2014) High Manganese and Aluminum Steels for the Military and Transportation Industry. *JOM* **66**, 1770–1784.

Fraś, E., Górny, M., & Lopez, H.F. (2007) Eutectic Cell and Nodule Count in Cast Iron Part I. Theoretical Background. *ISIJ Int.*, *47*, 259–268.

Stefanescu, D.M. (2015) *Science and Engineering of Casting Solidification*, 3rd ed.; Springer: Cham, Switzerland, ISBN 978-3-319-15692-7.

Boeri, R. & Sikora, J. (**2001**) Solidification macrostructure of spheroidal graphite cast iron. *J. Cast Met. Res. 13*, 307–313.

Natxiondo, A., Suárez, R., Sertucha, J., & Larrañaga, P. (2015) Graphite and Solid Fraction Evolutions during Solidification of Nodular Cast Irons. *Metals 5*, 239–255.

Fatahalla, N., AbuElEzz, A., Semeida, M. (2009) C, Si and Ni as alloying elements to vary carbon equivalent of austenitic ductile cast iron: Microstructure and mechanical properties. *Mater. Sci. Eng. A 504*, 81–89.

Górny, M., Kawalec, M., Sikora, G., & Lopez, H.F. (2014) Effect of Cooling Rate and Titanium Additions on Microstructure of Thin-Walled Compacted Graphite Iron Castings. *ISIJ Int. 54*, 2288–2293.

Llorca-Isern, N., Nesa, D., & Vicente, M. (2003) Thin wall compacted graphite cast iron for automotive applications. *Int. J. Cast. Metal. Res. 16*, 325–32

European Journal of Material Science 10 (1), 37-52, 2022
Print ISSN: ISSN 2055-6551(Print),
Online ISSN: ISSN 2055-656X (Online)
Website: https://www.eajournals.org/
Publication of the European Centre for Research Training and Development UK